Available online at www.sciencedirect.com

ScienceDirect

*Mendeleev Commun.*, 2021, **31**, 113–115

Mendeleev Communications

# Upconversion luminescence and ratiometric temperature sensing behavior of $Er^{3+}/Yb^{3+}$-codoped $CaY_2Ge_3O_{10}$ germanate

**Olga A. Lipina,* Ludmila L. Surat, Alexander Yu. Chufarov, Alexander P. Tyutyunnik and Vladimir G. Zubkov**

*Institute of Solid State Chemistry, Ural Branch of the Russian Academy of Sciences, 620990 Ekaterinburg, Russian Federation. E-mail: LipinaOlgaA@yandex.ru*

DOI: 10.1016/j.mencom.2021.01.035

**A new series of $CaY_{2-10x}Yb_{9x}Er_xGe_3O_{10}$ trigermanates (space group $P2_1/c$, $Z = 4$) has been synthesized using an EDTA-assisted method. Under 980 nm laser diode excitation, the samples exhibit intense upconversion luminescence corresponding to the characteristic transitions $^2H_{9/2} \rightarrow {}^4I_{15/2}$ (400–420 nm), $^2H_{11/2}, {}^4S_{3/2} \rightarrow {}^4I_{15/2}$ (500–600 nm) and $^4F_{9/2} \rightarrow {}^4I_{15/2}$ (625–725 nm) in $Er^{3+}$ ions. The $CaY_{1.5}Yb_{0.45}Er_{0.05}Ge_3O_{10}$ phosphor can be used as a good temperature sensor with high absolute and relative sensitivities $S_a(\max) = 0.0051\ K^{-1}$ and $S_r(\max) = 0.0109\ K^{-1}$.**

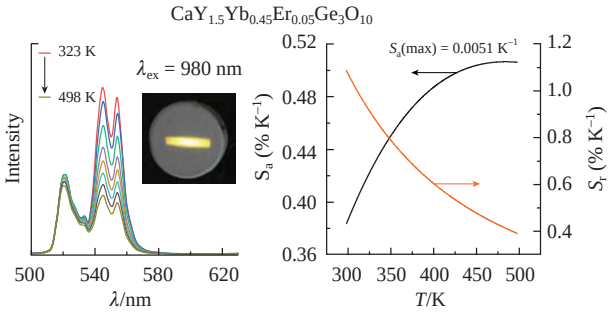


*Keywords*: luminescence, phosphors, temperature sensing, germanates, erbium.

Non-contact temperature measurement methods, which can be used for the diagnostics of material behaviors under adverse conditions of strong electromagnetic fields, high voltages, *etc.*, are of considerable current interest. These measurements can be conducted using special phosphors emitting under exciting radiation, and they are based on the thermal dependence of emission band shapes, the lifetime of excited states, or the fluorescence intensity ratio (FIR) of two bands in a spectrum.[1,2] The FIR concept is widely used for upconversion materials doped with lanthanide ions, whose electronic structure contains thermally coupled electronic energy levels.[3–7] The most common examples of such materials comprise $Yb^{3+}$ ions as a sensitizer and $Er^{3+}$, $Ho^{3+}$, or $Tm^{3+}$ ions as upconverter activators.[1] Recently a strong orange color emission under 980 nm excitation was revealed in $CaYb_{2-x}Er_xGe_3O_{10}$ trigermanates ($x = 0.1$–$2.0$) prepared using an ethylenediaminetetraacetic acid (EDTA) assisted route.[8] An optimum $Yb^{3+}/Er^{3+}$ ratio for the $CaYb_{2-x}Er_xGe_3O_{10}$ series was 9:1. However, since the total concentration of optical centers in the samples was excessive, there is a need to investigate related trigermanates with lower concentrations of $Yb^{3+}/Er^{3+}$ ions.

This work was focused on the upconversion luminescence and temperature-sensing performance of a $CaY_{2-10x}Yb_{9x}Er_xGe_3O_{10}$ ($x = 0.005$–$0.200$) family. The FIR of two bands associated with transitions from thermally coupled $^2H_{11/2}$ and $^4S_{3/2}$ levels in $Er^{3+}$ was studied as a function of temperature in a range of 298–498 K.

The compounds $CaY_{2-10x}Yb_{9x}Er_xGe_3O_{10}$ ($x = 0.005$, 0.015, 0.025, 0.05, 0.10, 0.15 and 0.20) were synthesized using an EDTA-assisted method at a sensitizer ($Yb^{3+}$)/activator ($Er^{3+}$) ratio of 9:1.[8,†] The sample morphology of $CaY_{1.5}Yb_{0.45}Er_{0.05}Ge_3O_{10}$ was studied by scanning electron microscopy (SEM) using a JEOL JSM–6390 LA microscope. It was found that the powder was formed by dense particles with irregular shapes and average sizes of 0.2–4.5 μm. A maximum of the log-normal distribution was observed at 1.3 μm (Figure S1).‡

According to the X-ray powder diffraction (XRPD) data,§ the $CaY_{2-10x}Yb_{9x}Er_xGe_3O_{10}$ ($x = 0.005$–$0.200$) series is isostructural with $CaY_2Ge_3O_{10}$.[9,10] The results of the Rietveld structural refinement[11–13] for $CaY_{1.5}Yb_{0.45}Er_{0.05}Ge_3O_{10}$ germanate are shown in Table S1 and Figure S2.‡ The final values of atomic positions, isotropic displacement parameters and occupations are listed in Table S2, and selected interatomic distances and bond angles are given in Table S3.‡

The crystal structure of the test germanates, space group $P2_1/c$ ($Z = 4$), consists of (001) layers of calcium and rare earth atoms connected through $[Ge_3O_{10}]^{8-}$ groups (Figure 1). The cation sublattice of the compounds possesses three nonequivalent Ca/Y/Yb/Er sites coordinated by seven oxygen atoms. One of them is almost fully ordered and contains mainly rare earth atoms; the fractions of calcium atoms in other two sites are close to 0.5 (Table S2).‡

† $CaCO_3$ (99.9%), $Y_2O_3$ (99.99%), $Yb_2O_3$ (99.99%), and $Er_2O_3$ (99.99%) taken in stoichiometric amounts were dissolved in 6 M $HNO_3$, and $GeO_2$ (99.5%) was dissolved in a 0.5 M aqueous solution of $NH_4OH$. The solutions were merged together, and then an appropriate amount of an $NH_4$–EDTA complexing agent was added. The mixture was evaporated at 90–95 °C until a dark grey powder-like residue was formed. The resulting precursor was heated at 200–800 °C in air to remove the organic component. The final annealing was performed at 1000, 1100, 1200 and 1250 °C with intermediate cooling and grinding at each stage.

‡ See details in Online Supplementary Materials.

§ The XRPD patterns were recorded on a STADI–P automated diffractometer (STOE) equipped with a linear mini–PSD detector. The data were collected in a transmission geometry using $CuK\alpha_1$ radiation over an angular range of $5° \leqslant 2\theta \leqslant 120°$ with a step of 0.02°. Polycrystalline silicon, $a = 5.43075(5)$ Å, was used as an external standard. The phase purity of the samples was checked by comparing their XRPD patterns

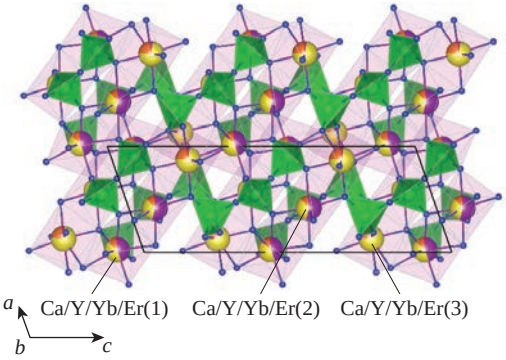


**Figure 1** Crystal structure of $CaY_{1.5}Yb_{0.45}Er_{0.05}Ge_3O_{10}$ illustrated along the [010] direction with $GeO_4$ tetrahedra (green) and $Ca/Y/Yb/ErO_7$ polyhedra (violet); Ca/Y/Yb/Er, Ge and O atoms are shown as violet/yellow/orange/red, green and blue balls, respectively.

Under 980 nm excitation, the $CaY_{2-10x}Yb_{9x}Er_xGe_3O_{10}$ trigermanates gave a strong upconversion emission visible to the naked eye (Figure 2, insets).¶ The emission color changed from green to orange with increasing dopant concentration; thus, the color characteristics of the phosphors can be varied by a proper selection of the chemical composition. The upconversion luminescence spectra of $CaY_{2-10x}Yb_{9x}Er_xGe_3O_{10}$ ($x$ = 0.015, 0.05 and 0.20) contain two main sets of lines at 500–600 and 625–725 nm corresponding to the $^2H_{11/2}$, $^4S_{3/2} \rightarrow {}^4I_{15/2}$ and $^4F_{9/2} \rightarrow {}^4I_{15/2}$ transitions in $Er^{3+}$ ions, respectively (Figure 2). A less intense peak at 408 nm caused by the $^2H_{9/2} \rightarrow {}^4I_{15/2}$ transition points to a high efficiency of energy transfer in the test compounds.

According to the concentration dependence, the highest emission intensity was reached in the $CaY_{1.5}Yb_{0.45}Er_{0.05}Ge_3O_{10}$ sample [Figure 3(*a*)]. The green to red intensity ratio ($R_{green/red}$) was calculated for the compounds based on integrated emission line intensities in ranges of 500–600 and 625–725 nm. Figure 3(*b*) shows that $R_{green/red}$ gradually decreased from 2.5 to 0.2 with the dopant concentration in the $CaY_{2-10x}Yb_{9x}Er_xGe_3O_{10}$ series.

In order to understand the number of pump photons involved in the UC mechanisms, we carried out excitation power dependence measurements. Since the upconversion emission intensity and the excitation power obey the relation

$$I(P) \propto P^n, \quad (1)$$

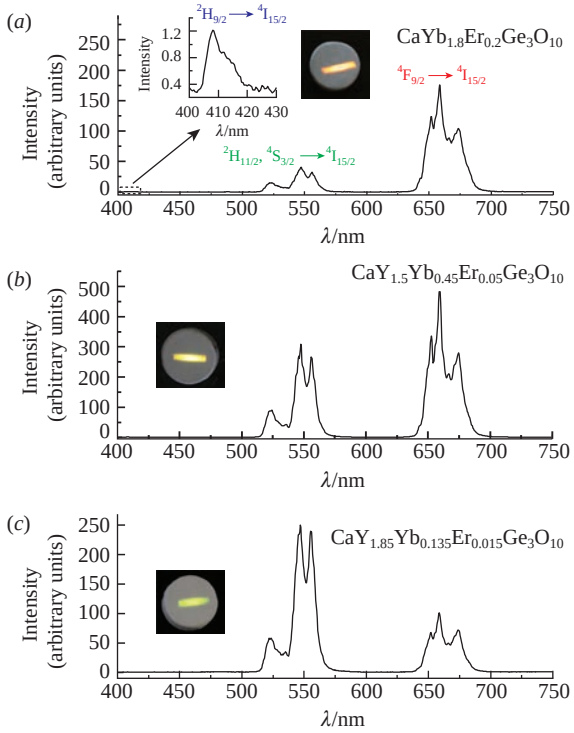


**Figure 2** Upconversion luminescence spectra of $CaY_{2-10x}Yb_{9x}Er_xGe_3O_{10}$ phosphors with $x$ equal to (*a*) 0.2, (*b*) 0.05 and (*c*) 0.015 ($\lambda_{ex}$ = 980 nm, $P$ = 2.7 W cm$^{-2}$). Insets: digital photographs of the fluorescence emission.

where $n$ is the number of NIR photons absorbed to excite one upconversion photon,[14] the slope of the log–log plot of UC emission intensity *versus* pump power gives the value of $n$.

Figure 3(*c*) shows the double logarithmic plots of upconversion emission intensity at the optimal dopant concentration $x$ = 0.05 as a function of excitation power. Both green and red emissions show a quadratic dependence on the excitation power in the low

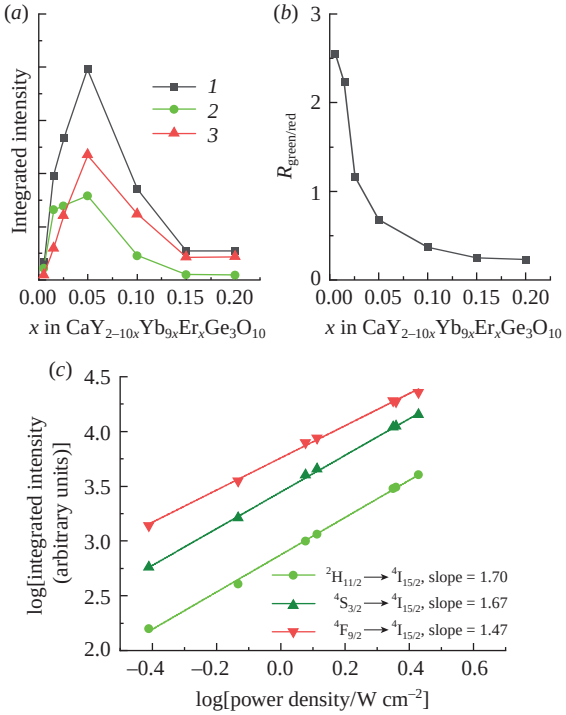


**Figure 3** (*a*) Evolution of integrated emission intensities (*1*) in the visible range, (*2*) at 500–600 nm, $^2H_{11/2}$, $^4S_{3/2} \rightarrow {}^4I_{15/2}$ transitions, (*3*) at 625–725 nm, $^4F_{9/2} \rightarrow {}^4I_{15/2}$. (*b*) $R_{green/red}$ as a function of $x$ in $CaY_{2-10x}Yb_{9x}Er_xGe_3O_{10}$ ($\lambda_{ex}$ = 980 nm). (*c*) The power dependence of upconversion luminescence intensity for the $CaY_{1.5}Yb_{0.45}Er_{0.05}Ge_3O_{10}$ sample in the low-power regime.

with those in the PDF2 database (ICDD, release 2016). The data for a representative $CaY_{1.5}Yb_{0.45}Er_{0.05}Ge_3O_{10}$ sample were analyzed by the Rietveld method, as implemented in the GSAS program suite. The previously reported data for $CaY_2Ge_3O_{10}$ were used as a starting model. The sum of the fractions of calcium and rare earth atoms was fixed at 1.0 using fractions constraints, and chemical restraints were used to keep the overall composition $CaY_{1.5}Yb_{0.45}Er_{0.05}Ge_3O_{10}$. A pseudo-Voigt function and a 36-term shifted Chebyshev polynomial were employed to model peak shapes and the background level, respectively.

*Crystal data for* $CaY_{1.5}Yb_{0.45}Er_{0.05}Ge_3O_{10}$. $M$ = 637.43, monoclinic, space group $P2_1/c$, at 273 K: $a$ = 6.89311(3), $b$ = 6.82566(3) and $c$ = 18.72812(9) Å, $\beta$ = 108.9708(3)°, $V$ = 833.298(8) Å$^3$, $Z$ = 4, and $d_{calc}$ = 5.081 g cm$^{-3}$. The number of measured reflections is 1235. $R_{wp}$ = 3.38%, $R_p$ = 2.52%, $R(F^2)$ = 1.37%. Further details of the crystal structure investigation may be found in Online Supplementary Materials or obtained from FIZ Karlsruhe, 76344 Eggenstein-Leopoldshafen, Germany (fax: +49 7247 808 666; e-mail: crysdata@fiz-karlsruhe.de) on quoting the deposition CSD number: 2021448.

¶ The room temperature upconversion luminescence spectra were recorded on a Varian Cary Eclipse fluorescence spectrometer using a 980 nm output of a laser diode ($P_{max}$ = 2.7 W cm$^{-2}$, KLM-H980-120-5). The laser power was controlled with an 11XLP12-3S-H2 Extreme Low Power Laser Detector (Standa). The temperature sensing properties at 298–498 K were studied using a Specac GS-21525 variable temperature cell holder and an MDR-204 monochromator (LOMO-Photonica) equipped with a PMT H10720C-01 high speed cooled (Hamamatsu).

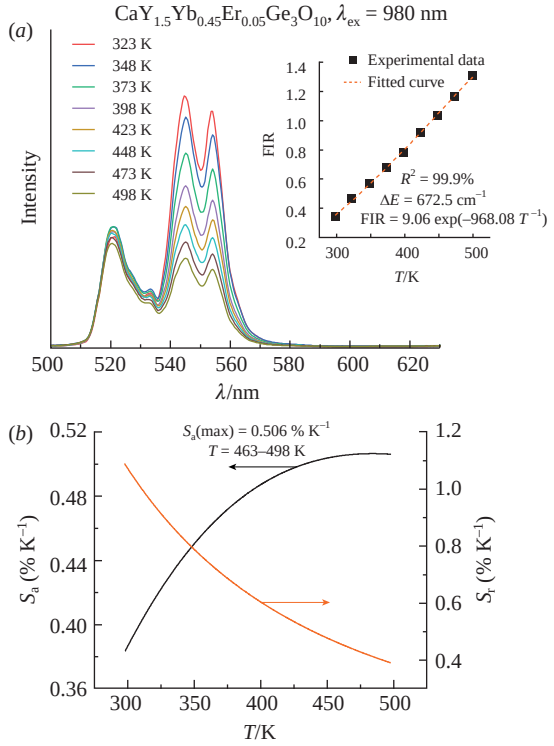


**Figure 4** (*a*) Upconversion luminescence spectra of phosphor $CaY_{1.5}Yb_{0.45}Er_{0.05}Ge_3O_{10}$ measured at different temperatures. Inset: the temperature dependence of FIR. (*b*) The absolute and relative sensitivities as functions of temperature.

power regime, which confirms that two-photon steps are involved. Thus, the possible excitation and de-excitation mechanisms for the studied trigermanates do not contradict the currently accepted standard model described by Auzel.[15]

Figure 4(*a*) illustrates the variation of the upconversion luminescence of $CaY_{1.5}Yb_{0.45}Er_{0.05}Ge_3O_{10}$ with temperature in a spectral range of 500–630 nm. The FIR of two emission bands at 521 and 554 nm associated with transitions from the excited thermal-coupled $^2H_{11/2}$ and $^4S_{3/2}$ states increased with temperature, and it can be approximated by the equation[1,2]

$$\mathrm{FIR} = B\exp\left(\frac{-\Delta E}{k_B T}\right), \quad (2)$$

where $B$ is a constant, $\Delta E$ is the energy gap between $^2H_{11/2}$ and $^4S_{3/2}$ levels, $T$ is absolute temperature, and $k_B$ is Boltzmann's constant. The experimental data are well fitted to the function FIR = 9.06 exp(–968.08 $T^{-1}$); the calculated $\Delta E$ is 672.5 cm$^{-1}$.

The absolute ($S_a$) and relative ($S_r$) thermal sensitivities are the most significant values calculated using the following equations:[1,2]

$$S_a = \frac{\mathrm{dFIR}}{\mathrm{d}T} = B\frac{\Delta E}{k_B T^2}\exp\left(\frac{-\Delta E}{k_B T}\right), \quad (3)$$

$$S_r = \frac{1}{\mathrm{FIR}}\frac{\mathrm{dFIR}}{\mathrm{d}T} = \frac{\Delta E}{k_B T^2}. \quad (4)$$

Figure 4(*b*) shows that the maximum values of $S_a$ = 0.0051 K$^{-1}$ and $S_r$ = 0.0109 K$^{-1}$ were reached at 463–498 and 298 K, respectively. These results are very close to that reported for $Al_2O_3$:$Yb^{3+}$, $Er^{3+}$.[16] The sensitivities achieved in this work exceed previously reported data for $Er^{3+}/Yb^{3+}$-codoped compounds such as α-$NaYF_4$:$Er^{3+}/Yb^{3+}$ and $Y_2SiO_5$:$Er^{3+}$, $Yb^{3+}$, but they are inferior to the values determined for Er–Mo:$Yb_2Ti_2O_7$ ($S_a$ = 0.0074 K$^{-1}$), $BaMoO_4$:$Er^{3+}/Yb^{3+}$ ($S_a$ = 0.0206 K$^{-1}$) and $SrWO_4$:$Er^{3+}/Yb^{3+}$ ($S_a$ = 0.015 K$^{-1}$).[3,6]

In summary, the $CaY_{2-10x}Yb_{9x}Er_xGe_3O_{10}$ ($x$ = 0.005–0.200) trigermanates were synthesized using an EDTA-assisted route, and their upconversion characteristics were estimated. The emission color of the phosphors can be changed from green to orange by adjusting the concentrations of $Yb^{3+}$ and $Er^{3+}$ dopant ions. The temperature sensing behavior of $CaY_{1.5}Yb_{0.45}Er_{0.05}Ge_3O_{10}$ was examined using the FIR technique for two green upconversion luminescence bands at 521 and 554 nm corresponding to the $^2H_{11/2} \rightarrow {}^4I_{15/2}$ and $^4S_{3/2} \rightarrow {}^4I_{15/2}$ transitions in $Er^{3+}$, respectively. The maximum sensitivities $S_a$ = 0.0051 K$^{-1}$ and $S_r$ = 0.0109 K$^{-1}$ indicate that the $CaY_{2-10x}Yb_{9x}Er_xGe_3O_{10}$ materials are promising for non-contact temperature sensors.

This work was supported by the Russian Science Foundation (grant no. 19-73-00219).

*Online Supplementary Materials*

Supplementary data associated with this article can be found in the online version at doi: 10.1016/j.mencom.2021.01.035.

## References

1 C. D. S. Brites, A. Millán and L. D. Carlos, in *Handbook on the Physics and Chemistry of Rare Earths*, eds. J. C. Bunzli and V. Pecharsky, Elsevier, 2016, vol. 49, ch. 281, pp. 339–427.
2 M. Dramićanin, *Luminescence Thermometry: Methods, Materials, and Applications*, Woodhead Publishing, 2018, ch. 6, pp. 113–157.
3 B. S. Cao, Y. Y. He, Z. Q. Feng, Y. S. Li and B. Dong, *Sens. Actuators, B*, 2011, **159**, 8.
4 B. Dong, B. Cao, Y. He, Z. Liu, Z. Li and Z. Feng, *Adv. Mater.*, 2012, **24**, 1987.
5 B. Dong, R. N. Hua, B. S. Cao, Z. P. Li, Y. Y. He, Z. Y. Zhang and O. S. Wolfbeis, *Phys. Chem. Chem. Phys.*, 2014, **16**, 20009.
6 X. Wang, Q. Liu, Y. Bu, C.-S. Liu, T. Liu and X. Yan, *RSC Adv.*, 2015, **5**, 86219.
7 B. S. Cao, Y. Bao, Y. Liu, J. Shang, Z. Zhang, Y. He, Z. Feng and B. Dong, *Chem. Eng. J.*, 2020, **385**, 123906.
8 O. A. Lipina, L. L. Surat, A. P. Tyutyunnik and V. G. Zubkov, *Opt. Mater.*, 2016, **61**, 98.
9 H. Yamane, R. Tanimura, T. Yamada, J. Takahashi, T. Kajiwara and M. Shimada, *J. Solid State Chem.*, 2006, **179**, 289.
10 O. A. Lipina, L. L. Surat, A. P. Tyutyunnik, I. I. Leonidov, E. G. Vovkotrub and V. G. Zubkov, *CrystEngComm*, 2015, **17**, 3333.
11 H. M. Rietveld, *J. Appl. Crystallogr.*, 1969, **2**, 65.
12 B. H. Toby, *J. Appl. Crystallogr.*, 2001, **34**, 210.
13 A. C. Larson and R. B. Von Dreele, *General Structure Analysis System (GSAS)*, Los Alamos, NM, 2004.
14 M. Pollnau, D. R. Gamelin, S. R. Lüthi, H. U. Güdel and M. P. Hehlen, *Phys. Rev. B*, 2000, **61**, 3337.
15 F. Auzel, *C. R. Acad. Sci. Paris*, 1966, **263**, 819.
16 B. Dong, D. P. Liu, X. J. Wang, T. Yang, S. M. Miao and C. R. Li, *Appl. Phys. Lett.*, 2007, **90**, 181117.

*Received: 11th August 2020; Com. 20/6285*